RESEARCH/REVIEW ARTICLE

Formation of Barents Sea Branch Water in the north-eastern Barents Sea

Vidar S. Lien[1] & Alexander G. Trofimov[2]

[1] Department of Oceanography, Institute of Marine Research, P.O. Box 1870, NO-5817 Bergen, Norway
[2] Knipovich Polar Research Institute of Marine Fisheries and Oceanography, 6 Knipovich Street, Murmansk, RU-183763, Russia

Keywords
Dense water formation; Kara Sea; deep water; Atlantic Water.

Correspondence
Vidar S. Lien, Department of Oceanography, Institute of Marine Research,
P.O. Box 1870, NO-5817 Bergen, Norway.
E-mail: vidar.lien@imr.no

Abstract

The Barents Sea throughflow accounts for approximately half of the Atlantic Water advection to the Arctic Ocean, while the other half flows through Fram Strait. Within the Barents Sea, the Atlantic Water undergoes considerable modifications before entering the Arctic Ocean through the St. Anna Trough. While the inflow area in the south-western Barents Sea is regularly monitored, oceanographic data from the outflow area to the north-east are very scarce. Here, we use conductivity, temperature and depth data from August/September 2008 to describe in detail the water masses present in the downstream area of the Barents Sea, their spatial distribution and transformations. Both Cold Deep Water, formed locally through winter convection and ice-freezing processes, and Atlantic Water, modified mainly through atmospheric cooling, contribute directly to the Barents Sea Branch Water. As a consequence, it consists of a dense core characterized by a temperature and salinity maximum associated with the Atlantic Water, in addition to the colder, less saline and less dense core commonly referred to as the Barents Sea Branch Water core. The denser core likely constitutes a substantial part of the total flow, and it is more saline and considerably denser than the Fram Strait branch as observed within the St. Anna Trough. Despite the recent warming of the Barents Sea, the Barents Sea Branch Water is denser than observed in the 1990s, and the bottom water observed in the St. Anna Trough matches the potential density at 2000 m depth in the Arctic Ocean.

The production of cold, dense water at high-latitude shelves plays an important role in the thermohaline circulation of the world's oceans (Meincke et al. 1997). In recent decades, a temperature increase in the Atlantic Water (AW) flow towards the Arctic Ocean has been observed (Quadfasel et al. 1991; Polyakov et al. 2005), and the temperature signal has been propagating downstream into the interior Arctic Ocean (Dmitrenko, Polyakov et al. 2008).

The poleward advection of AW along the Norwegian coast bifurcates at the entrance to the Barents Sea (Orvik & Niiler 2002). One branch, commonly called Fram Strait Branch Water (FSBW), continues northward along the western coast of Spitsbergen and eventually enters the Arctic Ocean through Fram Strait (Beszczynska-Möller et al. 2011). The other branch enters the Barents Sea (Skagseth et al. 2008), undergoes considerable modifications, and eventually enters the Arctic Ocean through the St. Anna Trough as Barents Sea Branch Water (BSBW; Schauer, Loeng et al. 2002).

The FSBW cools as it flows northward through the Fram Strait and downstream in the Nansen Basin it subducts below the cold halocline water in the Arctic Ocean and forms a subsurface temperature and salinity maximum (Rudels et al. 1999). Further downstream in the Arctic Ocean, some of the FSBW enters the Barents Sea from the north through various submarine valleys and canyons (Matishov et al. 2009; Lind & Ingvaldsen

Citation: *Polar Research* 2013, *32*, 18905, http://dx.doi.org/10.3402/polar.v32i0.18905

2012), both to the west of Franz Josef Land (Mosby 1938; Novitskiy 1967) and along the western flank of the St. Anna Trough (Hanzlick & Aagaard 1980; Loeng et al. 1993; Schauer, Loeng et al. 2002). The latter circulation pattern has also been suggested by geostrophic calculations (Panteleev et al. 2004), as well as by numerical model simulations (Kärcher et al. 2003; Gammelsrød et al. 2009). However, it is still unknown to what extent the FSBW influences the north-eastern Barents Sea. Hereinafter, we refer to the AW that is advected by the Barents Sea branch as Barents-derived Atlantic Water (bAW).

The Barents Sea is the largest shelf sea that is adjacent to the Arctic Ocean. It accounts for a substantial part of the dense water that is formed within the Arctic (Martin & Cavalieri 1989) and is therefore important for the renewal of the Intermediate and Deep Water in the Arctic Ocean (Rudels et al. 1994; Jones et al. 1995; Rudels et al. 2000). The continuous advection of warm AW keeps a substantial part of the Barents Sea ice-free year-round (Kvingedal 2005), resulting in a large net heat flux from the ocean to the atmosphere (Simonsen & Haugan 1996; Smedsrud et al. 2010). Several processes contribute to the modifications of the BSBW (Pfirman et al. 1994; Rudels et al. 1994; Ožigin & Ivšin 1999; Rudels et al. 2004). These processes include freshwater input from river runoff, sea-ice melting and net precipitation (Coachman & Barnes 1963; Steele et al. 1995), wind and tidal mixing (Sundfjord et al. 2007), atmospheric cooling and sea-ice formation (Aagaard et al. 1981; Jones & Anderson 1986). The formation of sea ice and the subsequent release of brine contribute to the formation of water masses with a density high enough to cause them to sink to great depths in the Arctic Ocean. Several of these dense water formation sites have been identified, including the Novaya Zemlya Bank (Nansen 1906; Midttun 1985; Ozhigin et al. 2000), the Great Bank, the Central Bank (Blindheim 1989; Loeng 1991), the Spitsbergen Bank (Sarynina 1969) and the area around Franz Josef Land (Martin & Cavalieri 1989). The BSBW, which is the downstream end product of wide-ranging modification processes, is commonly identified as an intermediate temperature and salinity minimum in the Θ-S space (Schauer, Rudels et al. 2002; Dmitrenko, Kirillov et al. 2008; Dmitrenko et al. 2009). However, our results challenge this traditional view.

The north-eastern Barents Sea is connected to the Arctic Ocean through the St. Anna Trough (Fig. 1). A 350-m-deep branch of the St. Anna Trough is oriented westward between Novaya Zemlya and Franz Josef Land. This branch will hereinafter be called the Western Trough. A saddle point with a sill depth of approximately

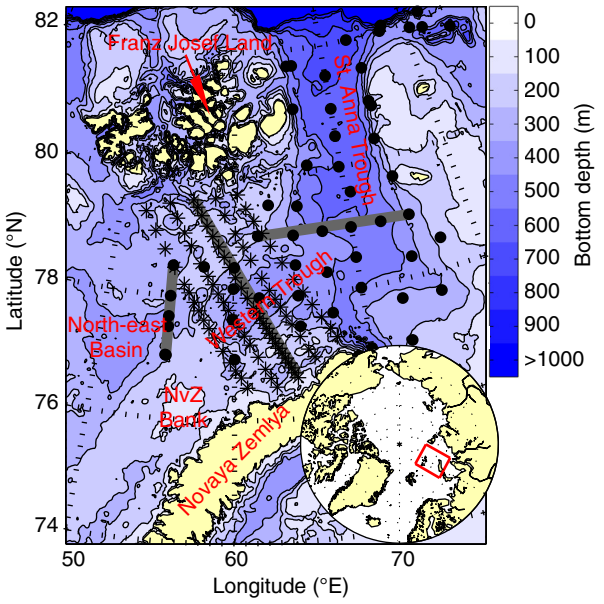

Fig. 1 Bathymetric map of the north-eastern Barents Sea and the St. Anna Trough. Stars show positions of stations obtained by the RV *Professor Boyko* and dots show positions of stations obtained by the RV *Obva*. Grey lines indicate discussed sections (see also Fig. 2).

200 m separates the Western Trough and the North-east Basin in the north-eastern Barents Sea. The depth of the St. Anna Trough varies between 300 and 500 m in the southern part and reaches 1000 m at the entrance to the Arctic Ocean in the north.

A portion of the recent Arctic climatic changes has been attributed to a multi-decadal oscillation within the North Atlantic (Sutton & Hodson 2005). The temperature variability in the Barents Sea is closely linked to this oscillation (Levitus et al. 2009), as observed in the Kola section (Tereščenko 1997); recent decades have constituted a warm phase (Skagseth et al. 2008). The thermohaline response to the temperature changes remains uncertain, although model studies indicate less dense water formation during warm periods (Årthun et al. 2011). Better knowledge of the formation, characteristics and subsequent export of Intermediate and Deep Water from the Barents Sea to the Arctic Ocean is therefore necessary.

Regular monitoring at the south-western entrance to the Barents Sea has revealed a recent increase in advected volume and heat into the Barents Sea (Skagseth et al. 2008). The outflow area to the north-east is, however, more irregularly and sparsely sampled, partly due to the seasonal ice coverage. As a consequence, little is known about the variability of the water masses flowing towards the Arctic Ocean. In this study, we present unique data that enable us to describe in detail the spatial distribution and characteristics of the water

Citation: *Polar Research* 2013, *32*, 18905, http://dx.doi.org/10.3402/polar.v32i0.18905

masses that are present at the doorstep to the Arctic Ocean. Furthermore, we track AW modifications through interaction with locally formed water masses en route to the Arctic Ocean by identifying the presence of various mixing processes, thereby adding to our existing knowledge of the exchanges between the Barents Sea and the Arctic Ocean.

Data and methods

Oceanic data

A total of 142 conductivity–temperature–depth (CTD) stations covering the St. Anna Trough and the north-eastern Barents Sea between Novaya Zemlya and Franz Josef Land were obtained during two cruises with the research vessels *Professor Boyko* and *Obva* (Fig. 1). The period covered was from late August to mid-September 2008. Although the merged data set spans a period of three weeks, we consider it to be synoptic due to our focus on the water masses below the pycnocline. The RV *Professor Boyko* was equipped with a FSI 3″ Micro CTD (Falmouth Scientific, Cataumet, MA, USA) and had a salinity accuracy of 0.0002 S/m and a temperature accuracy of 0.002°C. The RV *Obva* was equipped with a SBE 19 plus CTD system (Sea-Bird Electronics, Bellevue, WA, USA) and had a salinity accuracy of 0.0005 S/m and a temperature accuracy of 0.005°C. Some of the stations are combined into sections (Fig. 1): section A crosses the North-east Basin, section B crosses the Western Trough and section C crosses the St. Anna Trough at 79°N. In general, the St. Anna Trough is sparsely sampled, whereas the Western Trough is more densely sampled. However, based on the CTD measurements, we calculated an internal Rossby radius of approximately 1.5 km. Hence, most mesoscale features are not resolved by the CTD sampling.

Twenty-three CTD stations that covered section B were obtained in September 1991, using a Neil Brown CTD system (Neil Brown Ocean Sensors, Falmouth, MA, USA). The accuracy of the temperature sensor is 0.005°C, while the conductivity has an accuracy of 0.01.

Atmospheric data

Monthly averages of mean sea-level pressure, winds at a height of 10 m, and heat fluxes (sensible and latent heat and longwave and shortwave radiation) between the ocean and the atmosphere were obtained from the European Centre for Medium-Range Weather Forecasts ERA-Interim data set (Uppala et al. 2008), at a spatial resolution of $1.5^\circ \times 1.5^\circ$ for the period 1989–2008.

Results

Water mass characteristics

Three distinct water masses were present in the Western Trough during the observation period (Fig. 2), two of which were of Atlantic origin ($\Theta > 0$; see Table 1 for water mass definitions). The two water masses of Atlantic origin could be distinguished by their respective salinities. The water mass with the higher salinity corresponds to bAW. The water mass with the lower salinity was observed throughout the St. Anna Trough and had a temperature that decreased southwards, so we identified this water mass as FSBW. The third water mass was distinguished by its substantially lower temperature, with the lowest temperatures being close to the freezing point. Hereinafter, we will call this water mass Cold Deep Water (CDW). Although this was colder, the slightly lower salinity made it less dense than the bAW and only slightly denser than the FSBW. Hence, the bulk of the CDW was considered an intermediate water mass throughout the observation area.

Figures 3 and 4 demonstrate that the characteristics and depths of the different water masses vary geographically. Here, we have identified the core of each distinct water mass by the temperature extreme within the salinity range of the water mass (Fig. 2; Table 1). First and foremost, the different and only partly overlapping geographical distribution of bAW and FSBW is evident, as well as their respective downstream cooling: the bAW cools eastward while the FSBW cools south-westward in the St. Anna and Western troughs. In contrast, the CDW is heated where its presence overlaps with the bAW and/or FSBW. Furthermore, the sinking of the bAW and CDW into the Western and St. Anna troughs is evident. To further investigate the advection and modification of each water mass, vertical sections and Θ-S diagrams are described in the following section.

Re-circulating FSBW

FSBW enters the St. Anna Trough to the north-west (Fig. 1) and occupies the western and central areas (Fig. 3). This water has an intermediate temperature maximum (Figs. 2, 5, 6), with maximum temperatures of approximately 2°C in the inflow area. While the majority of FSBW circulates within the St. Anna Trough, one part enters the Western Trough and approximately follows the 200-m isobath (Fig. 6). In the Western Trough, the FSBW is identified as a warm core between approximately 50 m and 200 m depth, which is bounded above by cold Arctic Water and below by CDW. At this stage, the maximum temperature is

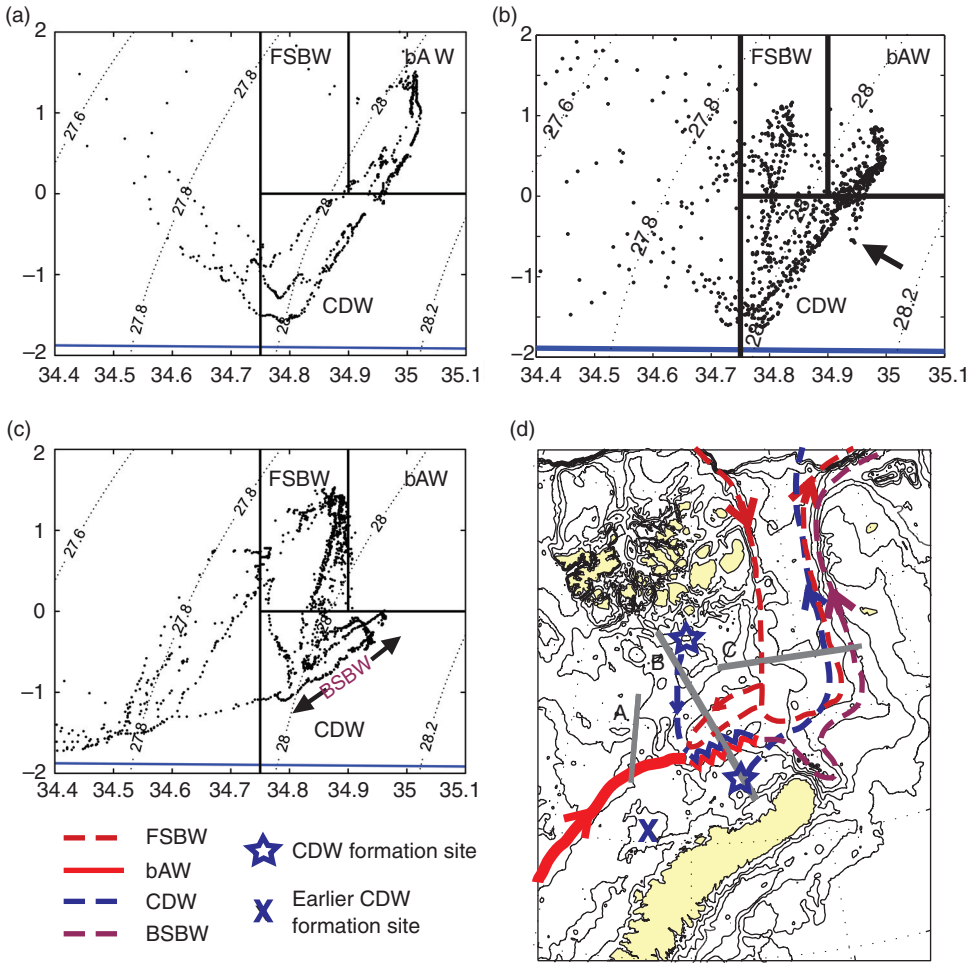

Fig. 2 Θ-S diagrams for the three sections: (a) A, (b) B and (c) C. Black lines indicate the bounds defining the different water masses: Fram Strait Branch Water (FSBW), Barents-derived Atlantic Water (bAW), Cold Deep Water (CDW) and Barents Sea Branch Water (BSBW). In (d), grey lines show positions of the sections and coloured lines show the advection paths of the different water masses. Blue lines in the Θ-S diagrams show the freezing temperature. The depth contours are similar to those in Fig. 1.

reduced to 1°C. While FSBW is clearly present in the Western Trough (Fig. 6), we found no trace of this water mass in the CTD data to the west of the saddle point separating the Western Trough and the North-east Basin (Fig. 2a).

Mixing between FSBW and CDW can be inferred from the Θ-S diagrams in both the Western Trough and the St. Anna Trough (Fig. 2), and mixing with surrounding water masses is also evident from the reduction in the FSBW temperature while en route. The mixing lines in the Θ-S diagrams indicate mostly isopycnal mixing. To investigate possible turbulent mixing, we estimated the gradient Richardson number following two slightly different procedures: the synoptic gradient Richardson number (Ri_s) assuming parallel flow, and the geostrophic gradient Richardson number (Ri_g) assuming geostrophic flow (van Gastel & Pelegrí 2004). A necessary condition for turbulence is then Ri_s, $Ri_g < 1$ (Abarbanel et al. 1984; Miles 1986). Following the suggestion by Loeng et al. (1997), we chose the surface as the level of no motion when calculating the geostrophic velocity. Based on the CTD data for section B, we found bottom-intensified currents along both the northern and southern slopes of the Western Trough (Fig. 7), with velocities comparable to those reported from direct current measurements (figure 6 in Gammelsrød et al. 2009). When calculating the synoptic gradient Richardson number, we assume that the section is perpendicular to the flow which is represented by the geostrophic velocity. Although we find local minima in the gradient Richardson number in the frontal areas of the FSBW, both the synoptic and geostrophic approaches yields Richardson numbers of O(10).

Citation: *Polar Research* 2013, *32*, 18905, http://dx.doi.org/10.3402/polar.v32i0.18905

Table 1 Water mass definitions. Barents Sea Branch Water may consist of both Cold Deep Water and Barents-derived Atlantic Water and has not been given any definite bounds here.

Water mass	Temperature range (°C)	Salinity range
Atlantic Water (AW)	$\Theta > 0$	$S > 34.75$
Fram Strait Branch Water (FSBW)	$\Theta > 0$	$34.75 < S < 34.9$
Barents-derived Atlantic Water (bAW)	$\Theta > 0$	$S > 34.9$
Cold Deep Water (CDW)	$\Theta < 0$	$S > 34.75$
Arctic Water	$\Theta < -1$	$34.3 < S < 34.7$
Surface Water (SW)	$\Theta > -1$	$S < 34.3$

Barents-derived Atlantic Water

bAW exits the Barents Sea through the North-east Basin and enters the Western Trough (Figs. 2, 3). Vertical profiles in the North-east Basin revealed two distinct layers, with warmer water overlying a colder, well-mixed layer. The two layers were separated by a thermocline located approximately at the sill depth of the connection between the North-east Basin and the Western Trough (not shown). While the two layers exhibit different temperatures, both layers have a similar salinity (35.0).

In the Western Trough, bAW occupies the southern slope and various banks on the Novaya Zemlya shelf (Fig. 6). It is also partly submerged under the CDW, creating a tilted front and horizontal density gradients between the two water masses, as well as a corresponding vertical velocity shear. By calculating the gradient Richardson number following the procedures above, we find values of O(10). Hence, the vertical velocity shear alone is not sufficient to overcome the stabilization by the stratification. In the deep part of the Western Trough, there is an indication of interleaving at the interface between the bAW and the CDW (Fig. 6, inset). The mixing with CDW reduces the temperature of the bAW from more than 1°C to approximately 0°C as it flows eastward from the North-east Basin, through the Western Trough and further downstream into the St. Anna Trough. The high salinity, however, is maintained due to the relatively high salinity in the CDW (Figs. 2, 3). In section C, a deep temperature maximum is seen within the CDW (Figs. 2, 5). Although it is below 0°C and therefore not categorized as bAW, the Θ-S properties clearly show its bAW origin. This suggests further cooling as the bAW continues through the St. Anna Trough (Fig. 2).

Cold Deep Water

Figure 2 documents the presence of CDW in the North-east Basin during the summer of 2008. The CDW spatial distribution was limited to the northern parts of the basin and the banks to the south of Franz Josef Land (Fig. 8). The core of the CDW was observed at intermediate depths, from just below the pycnocline at 50 m to approximately 150 m, with a minimum Θ of -1.6°C. The temperature increase with depth below this temperature minimum indicates an influence of water masses of Atlantic origin (bAW) from below (not shown). Hence, the winter convection during the preceding winter (2007/08) did not reach the bottom in the North-east Basin. This pattern is also evidenced by the lower potential density of the CDW compared to the bAW that is observed in the deeper parts of the North-east Basin (Fig. 2). Vertical profiles of temperature and salinity indicate the presence of double diffusive processes at the interface between the bAW and the overlying CDW at station 55 in section A (not shown).

In the Western Trough, eastward-flowing CDW forms an intermediate layer between the overlying FSBW and the underlying bAW (Fig. 6). As the CDW flows eastward, mixing with the surrounding water masses (Figs. 2, 3) increases the minimum potential temperature of the CDW from -1.6°C in the north-eastern Barents Sea to -0.6°C in the St. Anna Trough. While the CDW and the FSBW exhibit similar salinity, the bAW is more saline, which results in a slight increase in the CDW salinity.

Just north of Novaya Zemlya (Fig. 6, blue arrow) CDW with a higher potential temperature ($\Theta = -0.58$°C), higher salinity ($S = 34.95$) and higher potential density ($\sigma_\Theta = 28.09$) than the CDW observed in the North-east Basin was observed. This makes this water mass distinguishable in the Θ-S diagram (Fig. 2b, black arrow). A water mass with similar characteristics ($\Theta = -0.60$°C; $S = 34.94$) was observed in the bottom layer in the northern parts of the St. Anna Trough (not shown). No evidence of this water mass was observed between section B and the northern St. Anna Trough.

Air–sea interactions

A comparison of the net air-sea heat fluxes in the Barents Sea, which is based on the ERA-Interim data set during the winters of 1990/91 and 2007/08 and preceded the observations in summer 1991 and 2008, respectively, reveals substantial differences in the cooling pattern between the two periods (Fig. 9). During the winter of 2007/08, the most significant heat loss to the atmosphere occurred in the south-western quartile, compared to the winter of 1990/91, when the largest heat loss took place in the north-eastern quartile. Moreover, the general atmospheric circulation shows different patterns during the two winters. During the winter of 2007/08,

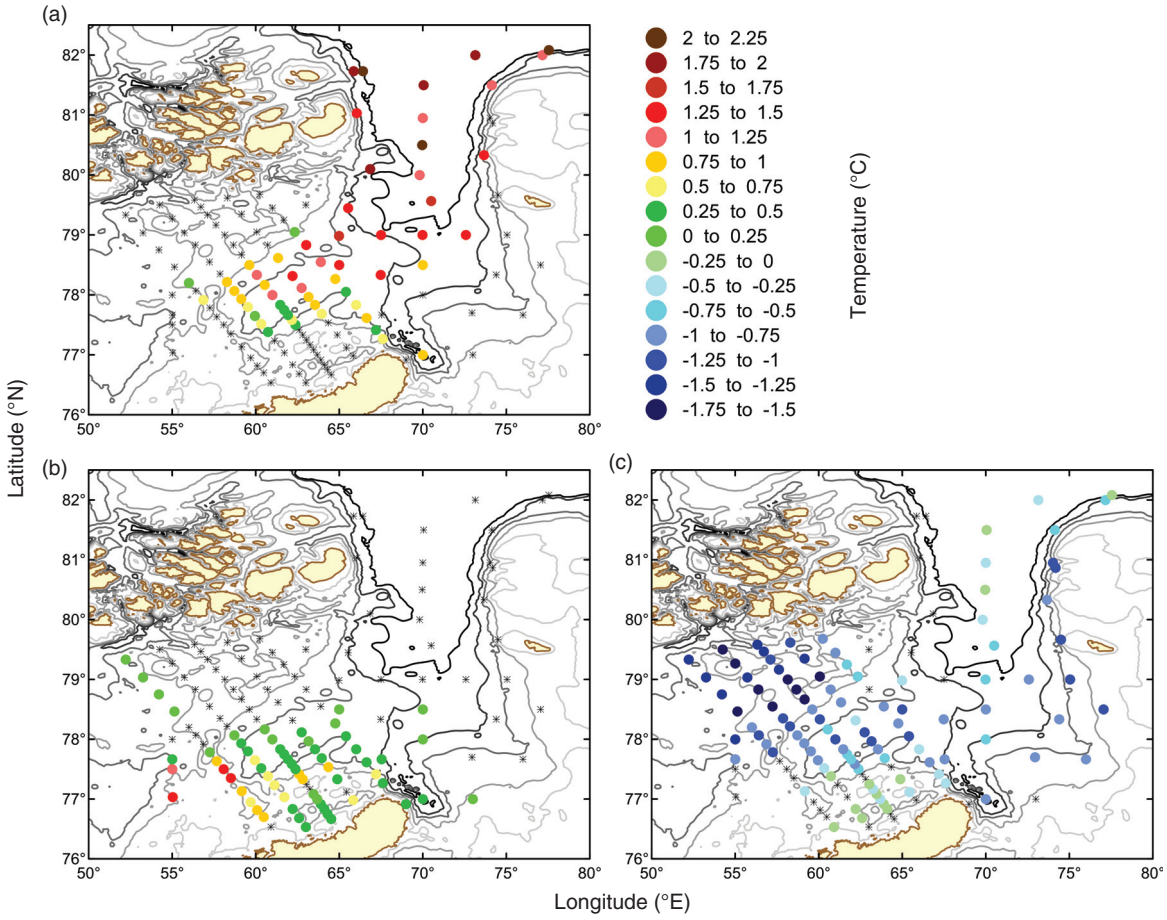

Fig. 3 Core water mass properties, represented by local maximum temperature (minimum temperature for Cold Deep Water) of the water masses discussed. The dots show the spatial distribution and the colour denote the respective core temperatures. (a) Recirculating Fram Strait Branch Water. (b) Barents-derived Atlantic Water. (c) Cold Deep Water. Depth contours similar to Fig. 1 are shown down to 500 m depth.

the Novaya Zemlya Bank was dominated by air masses from the south-west, whereas during the winter of 1990/91 the prevailing winds brought air masses from the south and east into the eastern Barents Sea.

Discussion

General circulation

Our interpretation of the general circulation pattern, which is based on the previously described observations, agrees with that of earlier studies (Schauer, Loeng et al. 2002; Rudels et al. 2004) and is summarized in Fig. 2. AW originating from the FSBW enters the St. Anna Trough from the north-west (Hanzlick & Aagaard 1980), while AW advected through the Barents Sea and cold water masses formed within the Barents Sea enter the St. Anna Trough from the south-west (Loeng et al. 1993; Schauer, Loeng et al. 2002). The salinity of the bAW exiting the Barents Sea into the Western Trough is close to the salinity of inflowing AW at the western entrance to the Barents Sea (Skagseth et al. 2008), implying that the bAW is formed mainly through direct atmospheric cooling of AW with only little input of freshwater. Our data clearly show that the flow of FSBW is topographically controlled and that it circulates within the St. Anna Trough and the Western Trough without entering the North-east Basin in the Barents Sea. However, the FSBW contributes to the modification of the BSBW en route to the Arctic Ocean.

The Θ-S diagrams from sections A, B and C (Fig. 2) show evidence of mixing between all three water masses observed within the Western Trough (bAW, FSBW and CDW). A calculation of both the synoptic and geostrophic gradient Richardson numbers based on the CTD data revealed values of O(10), which is one order of magnitude larger than the critical value (Abarbanel et al. 1984; Miles 1986), in the frontal areas between the different

Citation: *Polar Research* 2013, *32*, 18905, http://dx.doi.org/10.3402/polar.v32i0.18905

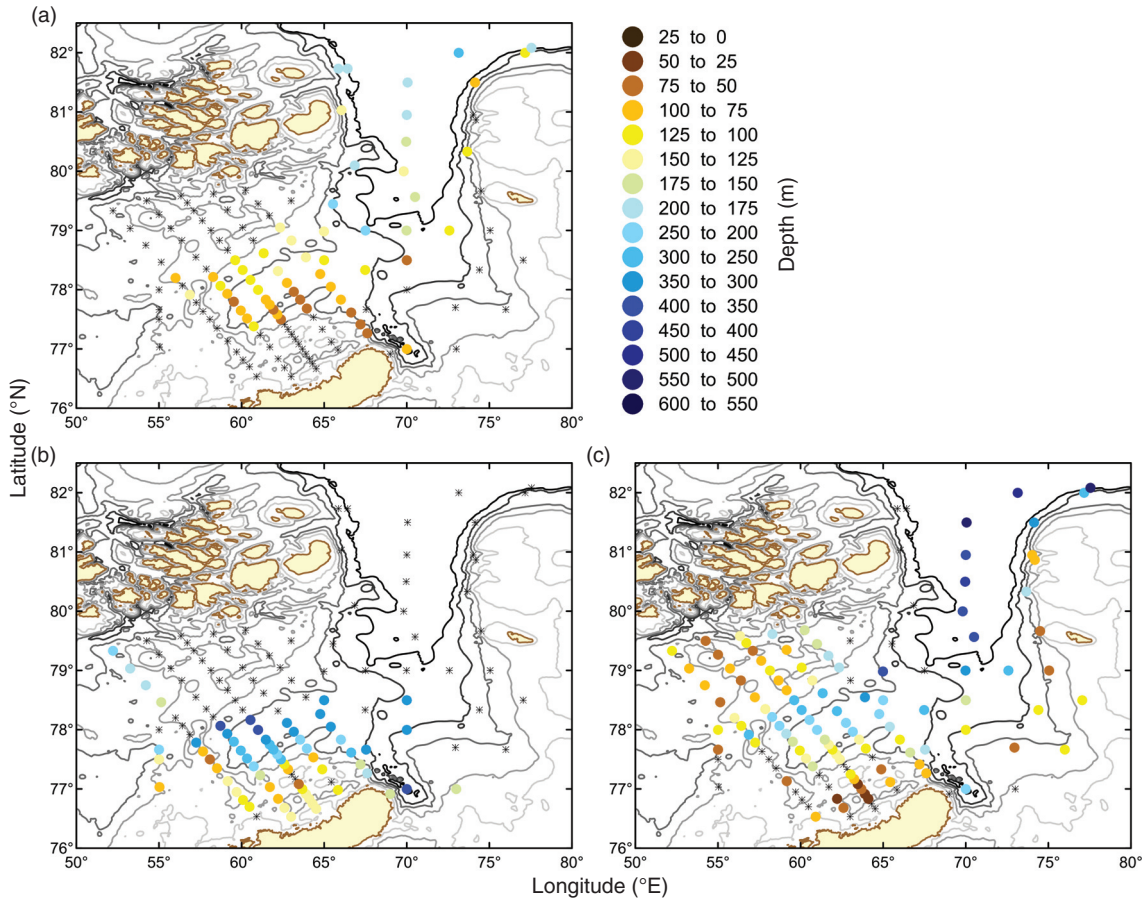

Fig. 4 Depth of water mass cores (see also Fig. 3), represented by maximum temperature (minimum temperature for Cold Deep Water) of the water masses discussed. The dots show the spatial distribution and the colour denote the respective core depths. (a) Recirculating Fram Strait Branch Water. (b) Barents-derived Atlantic Water. (c) Cold Deep Water. Depth contours similar to Fig. 1 are shown down to 500 m depth.

water masses considered here. However, based on direct current measurements and CTD observations from the Gulf Stream region, van Gastel & Pelegrí (2004) found that the geostrophic gradient Richardson number is always above the actual gradient Richardson number. Furthermore, van Gastel & Pelegrí (2004) argue that smoothing affect the calculated geostrophic gradient Richardson number, although the effect in the specific case considered was considered small. Here, we have used 5-m averages based on 1-m resolution data and the smoothing effect is therefore probably small. Despite these uncertainties, we conclude that the geostrophic vertical velocity shear alone, which is consistent with direct current measurements in section B in 1991 (figure 6 in Gammelsrød et al. 2009), is most likely not sufficiently strong to induce turbulent mixing. In the deepest part of the Western Trough, we find indications of interleaving in the frontal area between the bAW and the CDW. This represents another possible source of mixing, although the spacing between the CTD stations is too coarse to resolve such a process properly. The presence of double diffusive "staircases" in the North-east Basin suggests that double diffusive processes contribute to the vertical heat fluxes from the intermediate bAW to the overlying CDW here. Whereas Sundfjord et al. (2007) argue that double diffusive processes contribute significantly to vertical heat fluxes in frontal areas further west in the Barents Sea, our results suggest that this may also apply to the less energetic flow regime in the north-eastern parts of the Barents Sea. Moreover, our results may also imply that turbulent mixing plays the major role in the more energetic flow pattern downstream in the Western Trough and the St. Anna Trough, although the current dataset cannot substantiate any firm conclusions, but rather give some indications in terms of mixing processes.

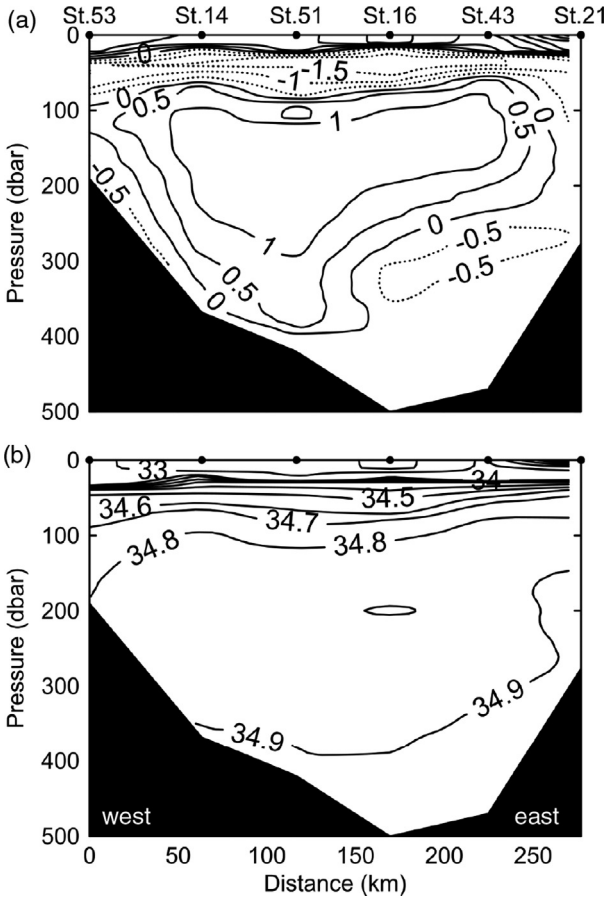

Fig. 5 Vertical sections of (a) potential temperature and (b) salinity in section C. Negative temperatures are shown by dotted lines.

Barents Sea Branch Water

Although our rigid water mass definitions implies that bAW is not present in the central and northern (not shown) parts of the St. Anna Trough, the Θ-S properties of the BSBW (Fig. 2; upper right) clearly shows that it originates partly from CDW and partly from cooled bAW. While the temperature and salinity minimum associated with the CDW part is commonly interpreted as the core of the BSBW within the Arctic Ocean (e.g., Schauer, Rudels et al. 2002; Dmitrenko et al. 2009), we argue that the deeper and denser ($28.0 < \sigma_\Theta < 28.08$) temperature and salinity maximum associated with the bAW part constitutes a core of Atlantic origin within the BSBW. Although we lack direct current measurements to quantify the relative contribution from the CDW and the bAW to the total flow from the Barents Sea towards the Arctic Ocean, we note that in 2008 the bAW occupied the part of section B (Fig. 6) where Gammelsrød et al. (2009) observed the strongest eastward current in 1991/92 (their figure 10). Our geostrophic calculations indicate that a similar flow pattern was present also in 2008. Hence, the relatively warm and saline core originating from the bAW, which was observed in the St. Anna Trough in 2008 likely constituted a substantial part of the BSBW flow towards the Arctic Ocean. Moreover, while the CDW-influenced part of the BSBW is both colder and less saline (but still denser) than the FSBW, as also noted by, e.g., Schauer, Rudels et al. (2002), we find that the bAW-influenced part is also colder but more saline and therefore considerably denser than the FSBW observed within the St. Anna Trough (σ_Θ ca. 27.9) and downstream in the Arctic Ocean (σ_Θ ca. 27.92; Dmitrenko et al. 2009).

Different modes of Cold Deep Water

At least two different CDW modes, with associated formation sites, were identified in our observations. The bulk of the CDW that was advected eastward into the Western Trough originated from the area immediately to the south-west of Franz Josef Land (Figs. 2–4). This CDW mode exhibited low potential temperatures that are associated with ice-freezing processes and relatively high salinities, although not high enough to achieve a potential density as high as the warmer, more saline bAW. This CDW mode formed an intermediate layer along the eastern rim of the St. Anna Trough.

A second CDW mode was observed on the shelf north of Novaya Zemlya (Figs. 2, 3), an area where polynyas regularly form, which enhances sea-ice production and subsequent brine release (Martin & Cavalieri 1989). The minimum potential temperature of -0.58°C shows that this CDW mode contains a relatively large bAW component but that its salinity is slightly lower than that of the bAW. The relatively fresh Novaya Zemlya Coastal Current (e.g., Jakobsen & Ozhigin 2011) is a likely source of the additional freshwater. When polynyas open where this CDW mode was observed, cold brine-enriched surface water descends through the underlying bAW and gains heat, thereby increasing its temperature. Model studies have shown that dense water formed on the Novaya Zemlya Bank is partly advected northward along the Novaya Zemlya coast (Årthun et al. 2011), while direct observations have shown that this water is advected south-westward and through the North-east Basin (Midttun 1985). Although we did not observe this CDW mode in the North-east Basin, the Novaya Zemlya Bank cannot be ruled out as its formation site. Nevertheless, based on the absence of this CDW mode in the North-east Basin, we speculate that this CDW mode was formed locally on the shelf immediately north of Novaya Zemlya. This mode had a higher potential density ($\sigma_\Theta = 28.09$) than the value ($\sigma_\Theta < 28.05$) reported

Citation: *Polar Research* 2013, *32*, 18905, http://dx.doi.org/10.3402/polar.v32i0.18905

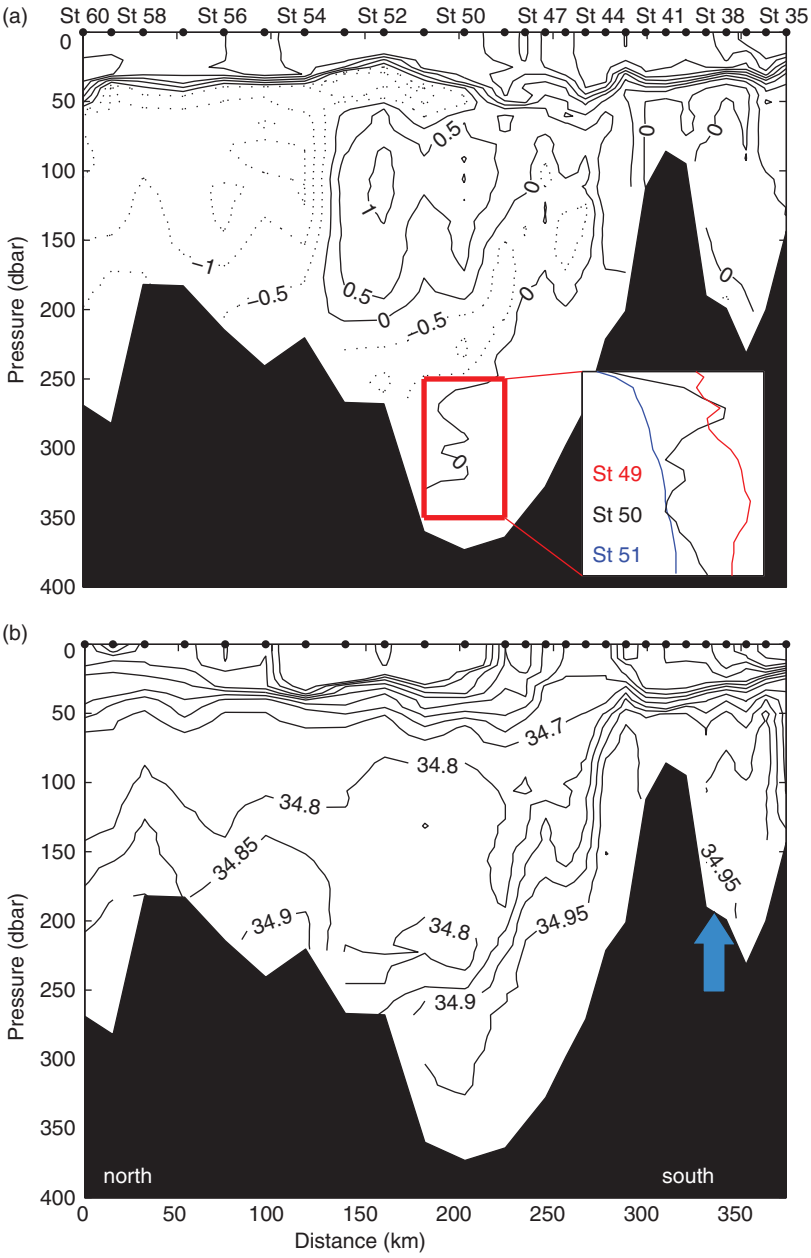

Fig. 6 Vertical sections of (a) potential temperature and (b) salinity in section B. Negative temperatures are shown by dotted lines. The blue arrow indicate dense Cold Deep Water mode in trench close to Novaya Zemlya. Inset: temperature profiles from stations 49–51 at 250–350 m depth (red box).

in 2002 (Schauer, Loeng et al. 2002) and was as high as that observed in 1965 (Hanzlick & Aagaard 1980). This indicates interannual variations in formation sites and characteristics of the different modes of CDW, although we lack data to draw any conclusions regarding their relative importance.

The similarity in the characteristics of the dense CDW observed to the north of Novaya Zemlya and in the northern parts of the St. Anna Trough suggests a common source. Although the area around Franz Josef Land regularly hosts active polynyas (Martin & Cavalieri 1989), we argue that the area to the north of Novaya Zemlya is a more likely, common source. According to Killworth (2001), density-driven plumes typically descend at a ratio of 1/400 relative to the along-isobath advection. Hence, a 300-m descent from 200 m (depth at the formation site) to 500 m (depth of the central St. Anna Trough) could be reached within an advection distance of approximately 120 km, which is shorter than the approximate distance of 450 km between the two

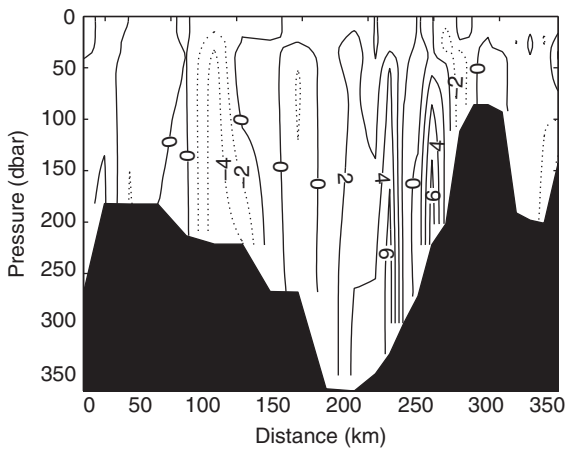

Fig. 7 Vertical section of geostrophic velocity in section B. Negative values are shown by dotted lines. Positive values toward the east.

observations sites. Thus, the bottom water observed in the northern parts of the St. Anna Trough might be remnants of a cascading outflow of the dense bottom water that was produced on the shelf north of Novaya Zemlya during the previous winter. The absence of this water mass further south in section C suggests a pulsating pattern of outflow and that most of the dense CDW had already descended into the Arctic Ocean by the time of the observations, although this could also be partly explained by sparse sampling coverage.

Interannual variability

There is a substantial difference between the bAW properties that were observed in 1991 (figure 2 in Gammelsrød et al. 2009) and those that were observed in 2008 (Fig. 2). The maximum temperature was 0.5°C warmer in 2008, and bAW and CDW were clearly identifiable in the Western Trough. In 1991, the characteristics of the eastward flowing water masses in the Western Trough were more similar to what was observed further downstream in the St. Anna Trough in 2008. One possible explanation is changes in the characteristics of the AW entering the Barents Sea in the south-west, which vary between years and decades (e.g., Skagseth et al. 2008) and thereby precondition the formation of CDW (Midttun & Loeng 1987). However, the varying sea-ice cover and subsequent changes in the air-sea heatfluxes within the Barents Sea tend to absorb the variability in the upstream conditions (Smedsrud et al. 2010; Årthun et al. 2012). We speculate that a more likely explanation is that the CDW formed at different sites in 1991 and 2008 due to the different cooling patterns in the preceding winters (Fig. 9). The pattern in 2008 was close to the climatological state, while the pattern in 1991 was clearly anom-

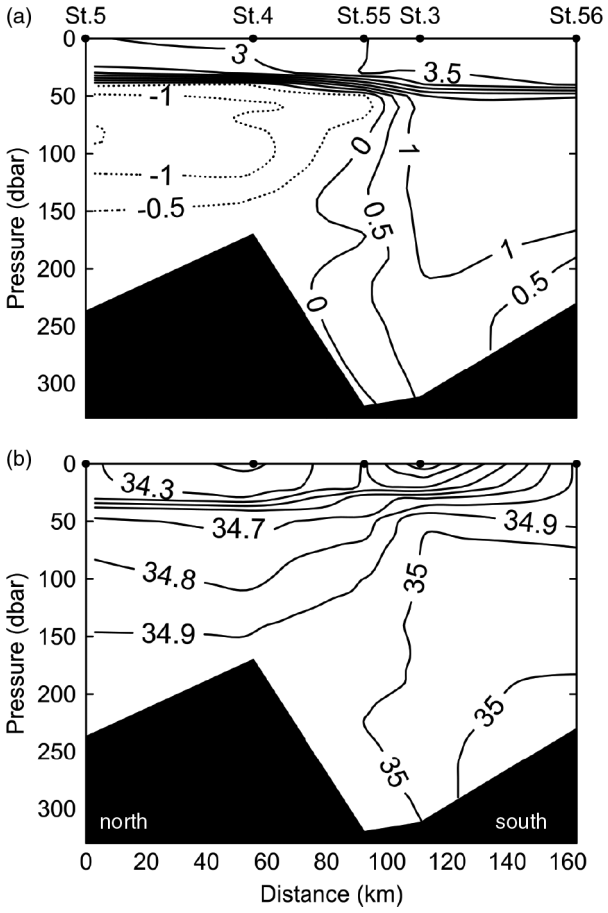

Fig. 8 Vertical sections of (a) potential temperature and (b) salinity in section A. Negative temperatures are shown by dotted lines.

alous compared to climatological values (e.g., Årthun & Schrum 2010). Based on this observation, we find it likely that substantial CDW production took place on the Novaya Zemlya Bank in 1991, as CDW was the dominating water mass over the bank and in the North-east Basin (not shown), as opposed to 2008 when no CDW was observed in that area. Indeed, in addition to advecting cold and dry air from the south-east, the more easterly prevailing winds during the winter of 1990/91 favoured polynya activity, to a large extent, on the Novaya Zemlya Bank (Fig. 9c). In contrast, relatively warm air masses were advected into the Barents Sea from the south-west during the winter of 2007/08, which is reflected by the substantially lower temperatures on the Novaya Zemlya Bank in the winter of 1990/91 compared to 2007/08 (Fig. 9c, d). A south-westward shift in the main CDW production site in 1991 compared to 2008 would force the CDW to encounter the bAW further upstream, whereas in 2008, the two water masses were kept more or less separated until they entered the Western Trough. The modelled north-eastward advection path of CDW

Citation: *Polar Research* 2013, *32*, 18905, http://dx.doi.org/10.3402/polar.v32i0.18905

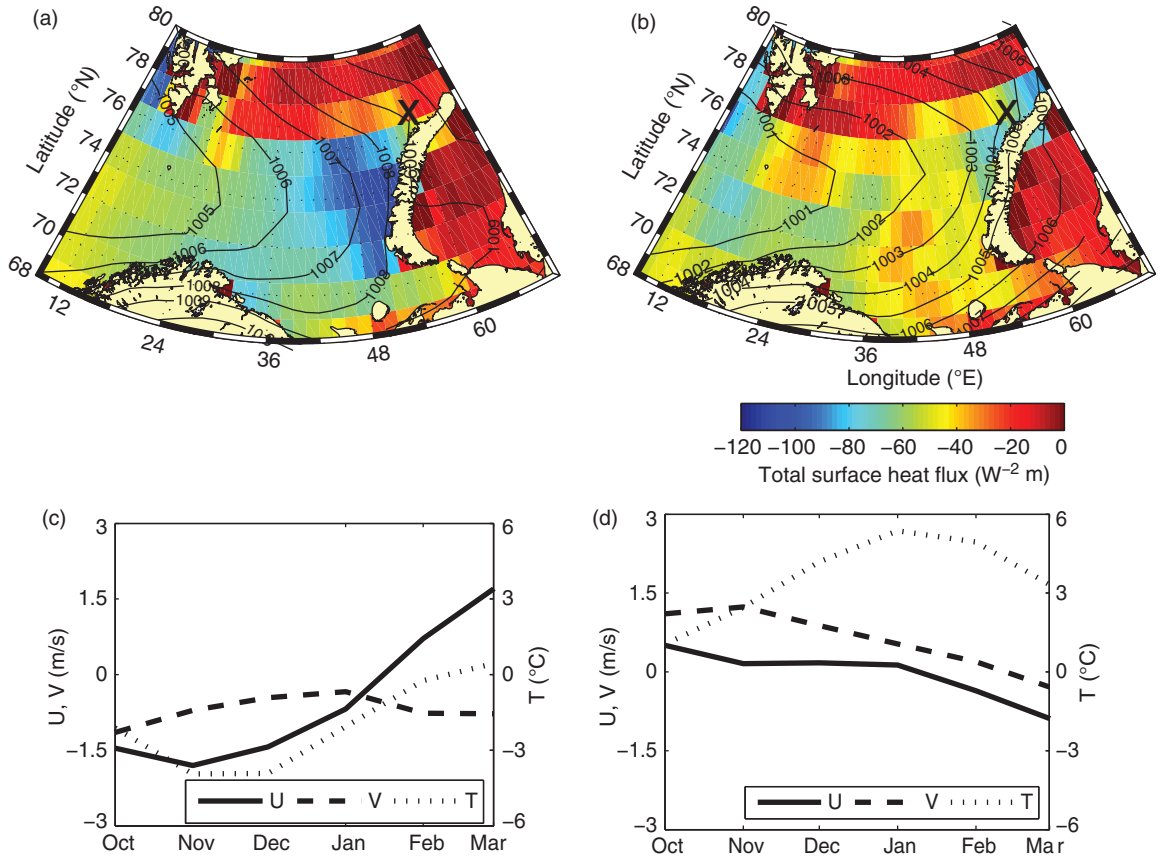

Fig. 9 Total heat fluxes between the ocean and the atmosphere (positive downwards) through the periods (a) October 1990 through March 1991 and (b) October 2007 through March 2008. X marks the sampling location on the Novaya Zemlya Bank. Lines show the mean sea level pressure (hPa) averaged over the same period. In (c) and (d), u- and v-wind velocity components and temperature at the location on the Novaya Zemlya Bank are shown.

formed on the Novaya Zemlya Bank (Årthun et al. 2011) suggests that a northward shift in the formation area forces a larger fraction of the CDW to enter the Western Trough directly and not flow south-westward and through the North-east Basin. The larger heat fluxes to the north of Novaya Zemlya in 2007/08 compared to 1991/90 further suggest that there was less ice cover in 2007/08 and therefore greater dense water production through direct atmospheric cooling.

Despite the recent warming of the AW flowing through the Barents Sea (Skagseth et al. 2008), we find evidence of the presence of bottom water flowing towards the Arctic Ocean that, according to figure 6 in Rudels et al. (2000), matches the potential density at 2000 m depth in the Arctic Ocean. Therefore, depending on the entrainment of surrounding water masses, the BSBW may potentially sink to greater depths than the 1300 m observed by Schauer et al. (1997). This sinking ventilates the deep water masses, although we lack adequate data to quantify the amount of this dense water mass. Moreover, the AW flowing through the Barents Sea is cooled to below 0°C before entering the Arctic Ocean. Hence, if −0.1°C is used as an overall temperature estimate of all water masses leaving the Arctic Ocean, as was proposed by Aagaard and Greisman (1975), it may be argued that the Barents Sea does not contribute to any heat gain in the Arctic Ocean, despite the recent warm period.

Concluding remarks

Based on an extensive, near-synoptic array of CTD measurements, we find that both water masses formed locally through ice freezing and thermohaline convective processes as well as AW modified through atmospheric cooling in the Barents Sea contribute directly to the BSBW observed in the St. Anna Trough. The two are identifiable within the BSBW by their different thermohaline characteristics as an intermediate temperature and salinity minimum and a deeper temperature and salinity maximum, respectively. As a result, the BSBW displays

a relatively wide density range ($28.0 < \sigma_\Theta < 28.09$). The densest part matches the potential density at 2000 m depth in the Arctic Ocean. The Barents Sea ice cover in winter has been reduced due to recent warming. This allows for more direct atmospheric cooling of the AW, while the freshwater input from ice melt has been reduced. As a consequence, the warm and saline, yet dense Atlantic origin part of the BSBW likely constitutes a substantial part of the total flow from the Barents Sea towards the Arctic Ocean. However, direct current measurements are required in order to determine the relative contribution and the variability of the water masses forming the BSBW. Additionally, turbulence measurements are needed in order to investigate the relative importance of the various mixing processes indicated here. Hence, there is a need for further research activity in this area.

Acknowledgements

The comments and suggestions of two anonymous reviewers, which helped improve the manuscript, are acknowledged. The Research Council of Norway through the International Polar Year (IPY) project Bipolar Atlantic Thermohaline Circulation (grant no. 176082, IPY cluster no. 23) has supported this work. Ilker Fer and Ken Drinkwater are acknowledged for constructive comments on an earlier version of the manuscript. We would also like to thank Øystein Skagseth for fruitful discussions. We wish to thank the captains and crews on-board the RV *Professor Boyko* and the RV *Obva* for their good cooperation and hospitality.

References

Aagaard K., Coachman L.K. & Carmack E.C. 1981. On the halocline of the Arctic Ocean. *Deep-Sea Research Part I 28*, 529–545.

Aagaard K. & Greisman P. 1975. Toward new mass and heat budgets for the Arctic Ocean. *Journal of Geophysical Research 80*, 3821–3827.

Abarbanel H.D.I., Holm D.D., Mardsen J.E. & Ratiu R. 1984. Richardson number criterion for the nonlinear stability of three-dimensional stratified flow. *Physical Review Letters 52*, 2352–2355.

Årthun M., Eldevik T., Smedsrud L.H., Skagseth Ø. & Ingvaldsen R.B. 2012. Quantifying the influence of Atlantic heat on Barents Sea ice variability and retreat. *Journal of Climate 25*, 4736–4743.

Årthun M., Ingvaldsen R.B., Smedsrud L.H. & Schrum C. 2011. Dense water formation and circulation in the Barents Sea. *Deep-Sea Research Part I 58*, 801–817.

Årthun M. & Schrum C. 2010. Ocean surface heat flux variability in the Barents Sea. *Journal of Marine Systems 83*, 88–98.

Beszczynska-Möller A., Woodgate R.A., Lee C., Melling H. & Karcher M. 2011. A synthesis of exchanges through the main oceanic gateways to the Arctic Ocean. *Oceanography 24*, 82–99.

Blindheim J. 1989. Cascading of Barents Sea bottom water into the Norwegian Sea. *Rapports et Procès-Verbaux des Réunions. Conseil Permanent International pour L'Exploration de la Mer 188*, 49–58.

Coachman L.K. & Barnes C.A. 1963. Surface waters in the Eurasian Basin of the Arctic Ocean. *Arctic 15*, 251–277.

Dmitrenko I.A., Bauch D., Kirillov S.A., Koldunov N., Minnett P.J., Ivanov V.V., Höleman J.A. & Timokhov L.A. 2009. Barents Sea upstream events impact the properties of Atlantic Water inflow into the Arctic Ocean: evidence from 2005 to 2006 downstream observations. *Deep-Sea Research Part I 56*, 513–527.

Dmitrenko I.A., Kirillov S.A., Ivanov V.V. & Woodgate R. 2008. Mesoscale Atlantic Water eddy off the Laptev Sea continental slope carries the signature of upstream interaction. *Journal of Geophysical Research—Oceans 113*, C07005, doi: 10.1029/2007JC004491.

Dmitrenko I.A., Polyakov I.V., Kirillov S.A., Timokhov L.A., Frolov I.E., Sokolov V.T., Simmons H.L., Ivanov V.V. & Walsh D. 2008. Toward a warmer Arctic Ocean: spreading of the early 21st century Atlantic Water warm anomaly along the Eurasian Basin margins. *Journal of Geophysical Research—Oceans 113*, C05023, doi: 10.1029/2007JC004158.

Gammelsrød T., Leikvin Ø., Lien V., Budgell W.P., Loeng H. & Maslowski W. 2009. Mass and heat transports in the NE Barents Sea: observations and models. *Journal of Marine Systems 75*, 56–69.

Hanzlick D. & Aagaard K. 1980. Freshwater and Atlantic Water in the Kara Sea. *Journal of Geophysical Research—Oceans and Atmospheres 85*, 4937–4942.

Jakobsen T. & Ozhigin V.K. 2011. *The Barents Sea—ecosystem, resources, management*. Trondheim: Tapir Academic Press.

Jones E.P. & Anderson L.G. 1986. On the origin of the chemical properties of the Arctic Ocean halocline. *Journal of Geophysical Research—Oceans 91*, 10759–10767.

Jones E.P., Rudels B. & Anderson L.G. 1995. Deep waters of the Arctic Ocean: origins and circulation. *Deep-Sea Research Part I 42*, 737–760.

Kärcher M., Kulakov M., Pivovarov S., Schauer U., Kauker F. & Schlitzer R. 2003. Atlantic Water flow to the Kara Sea: comparing model results with observations. In R. Stein et al. (eds.): *Siberian River run-off in the Kara Sea: characterisation, quantification, variability and environmental significance*. Pp. 47–69. Amsterdam: Elsevier.

Killworth P.D. 2001. On the rate of descent overflows. *Journal of Geophysical Research—Oceans 106*, 22267–22275.

Kvingedal B. 2005. Sea-ice extent and variability in the Nordic seas, 1967–2002. In H. Drange (ed.): *The Nordic seas: an integrated perspective*. Pp. 39–50. Washington, DC: American Geophysical Union.

Levitus S., Matishov G., Seidov D. & Smolyar I. 2009. Barents Sea multidecadal variability. *Geophysical Research Letters 36*, L19604, doi: 10.1029/2009GL039847.

Citation: *Polar Research* 2013, *32*, 18905, http://dx.doi.org/10.3402/polar.v32i0.18905

Lind S. & Ingvaldsen R.B. 2012. Variability and impacts of Atlantic Water entering the Barents Sea from the north. *Deep-Sea Research Part I 62*, 70–88.

Loeng H. 1991. Features of the physical oceanographic conditions of the Barents Sea. *Polar Research 10*, 5–18.

Loeng H., Ozhigin V. & Ådlandsvik B. 1997. Water fluxes through the Barents Sea. *ICES Journal of Marine Science 54*, 310–317.

Loeng H., Ozhigin V., Ådlandsvik B. & Sagen H. 1993. *Current measurements in the northeastern Barents Sea. ICES CM 1993/C:41*. Copenhagen: International Council for the Exploration of the Sea.

Martin S. & Cavalieri D.J. 1989. Contributions of the Siberian shelf polynyas to the Arctic Ocean intermediate and Deep Water. *Journal of Geophysical Research—Oceans 94*, 12725–12738.

Matishov G.G., Matishov D.G. & Moiseev D.V. 2009. Inflow of Atlantic-origin waters to the Barents Sea along glacial troughs. *Oceanologia 51*, 321–340.

Meincke J., Rudels B. & Friedrich H.J. 1997. The Arctic Ocean–Nordic seas thermohaline circulation. *ICES Journal of Marine Science 54*, 283–299.

Midttun L. 1985. Formation of dense bottom water in the Barents Sea. *Deep-Sea Research Part I 32*, 1233–1241.

Midttun L. & Loeng H. 1987. Climatic variations in the Barents Sea. In H. Loeng (ed.): *The effect of oceanographic conditions on the distribution and population dynamics of commercial fish stocks in the Barents Sea. Proceedings of the third Soviet–Norwegian Symposium, Murmansk, 26–28 May 1986*. Pp. 13–28. Bergen: Institute of Marine Research.

Miles J.W. 1986. Richardson's criterion for the stability of stratified shear flow. *Physics of Fluids 29*, 3470–3471.

Mosby H. 1938. *Svalbard waters. Geofysiske Publikasjoner 12(4)*. Bergen: Norwegian Geophysical Society.

Nansen F. 1906. *Northern waters: Captain Roald Amundsen's oceanographic observations in the Arctic seas in 1901. Vitenskabs-Selskabets Skrifter 1, Mathematisk-Naturvitenskapelig Klasse 3*. Christiania: Jacob Dybwad.

Novitskiy V.P. 1967. *Permanent currents of the northern Barents Sea. Naval Oceanographic Office Translation Vol. 349*. Washington, DC: US Naval Oceanographic Office.

Orvik K.A. & Niiler P. 2002. Major pathways of Atlantic water in the northern North Atlantic and Nordic seas toward Arctic. *Geophysical Research Letters 29*, article no. 1896, doi: 10.1029/2002GL015002.

Ožigin V.K. & Ivšin V.A. 1999. *Vodnye massy Barenceva Morja. (Water masses of the Barents Sea.)* Murmansk: Knipovich Polar Research Institute of Marine Fisheries and Oceanography.

Ozhigin V.K., Trofimov A.G. & Ivshin V.A. 2000. *The eastern basin water and currents in the Barents Sea. ICES CM 2000/L: 14*. Copenhagen: International Council for the Exploration of the Sea.

Panteleev G., Ikeda M., Grotov A., Nechaev D. & Yaremchuk M. 2004. Mass, heat and salt balances in the eastern Barents Sea obtained by inversion of hydrographic section data. *Journal of Oceanography 60*, 613–623.

Pfirman S.L., Bauch D. & Gammelsrød T. 1994. The northern Barents Sea: water mass distribution and modification. In O.M. Johannessen et al. (eds.): *The polar oceans and their role in shaping the global environment.* Pp. 77–94. Washington, DC: American Geophysical Union.

Polyakov I., Beszczynska A., Carmack E., Dmitrenko E., Fahrbach E., Frolov I., Gerdes R., Hansen E., Holfort J., Ivanov V., Johnson M., Kärcher M., Kauker F., Morison J., Orvik K., Schauer U., Simmons H., Skagseth Ø., Sokolov V., Steele M., Timokhov L., Walsh D. & Walsh J. 2005. One more step toward a warmer Arctic. *Geophysical Research Letters 32*, L17605, doi: 10.1029/2005GL023740.

Quadfasel D., Sy A., Wells D. & Tunik A. 1991. Warming in the Arctic. *Nature 350*, 385.

Rudels B., Friedrich H.J. & Quadfasel D. 1999. The Arctic circumpolar boundary current. *Deep-Sea Research Part II 46*, 1023–1062.

Rudels B., Jones E.P., Anderson L.G. & Kattner G. 1994. On the intermediate depth waters of the Arctic Ocean. In O.M. Johannessen et al. (eds.): *The polar oceans and their role in shaping the global environment.* Pp. 33–46. Washington, DC: American Geophysical Union.

Rudels B., Jones E.P., Schauer U. & Eriksson P. 2004. Atlantic sources of the Arctic Ocean surface and halocline waters. *Polar Research 23*, 181–208.

Rudels B., Muench R.D., Gunn J., Schauer U. & Friedrich H.J. 2000. Evolution of the Arctic boundary current north of the Siberian shelves. *Journal of Marine Systems 25*, 77–99.

Sarynina R.N. 1969. Conditions of origin of cold deep-sea waters in the Bear Island Channel. Paper presented at the Symposium on Physical Variability in the North Atlantic. 23–27 September, Dublin.

Schauer U., Loeng H., Rudels B., Ozhigin V.K. & Dieck W. 2002. Atlantic water inflow through the Barents and Kara Seas. *Deep Sea Research Part I 49*, 2281–2298.

Schauer U., Muench R.D., Rudels B. & Timokhov L. 1997. Impact of eastern Arctic shelf waters on the Nansen Basin intermediate layers. *Journal of Geophysical Research—Oceans 102*, 3371–3382.

Schauer U., Rudels B., Jones E.P., Anderson L.G., Muench R.D., Bjørk G., Swift J.H., Ivanov V. & Larsson A.-M. 2002. Confluence and redistribution of Atlantic water in the Nansen, Amundsen and Makarov basins. *Annales Geophysicae 20(2)*, 257–273.

Simonsen K. & Haugan P.M. 1996. Heat budgets of the Arctic Mediterranean and sea surface heat flux parameterizations for the Nordic seas. *Journal of Geophysical Research—Oceans 101*, 6553–6576.

Skagseth Ø., Furevik T., Ingvaldsen R., Loeng H., Mork K.A., Orvik K.A. & Ozhigin V. 2008. Volume and heat transports to the Arctic via the Norwegian and Barents seas. In R. Dickson et al. (eds.): *Arctic–Subarctic ocean fluxes: defining the role of the northern seas in climate.* Pp. 45–64. Dordrecht: Springer.

Smedsrud L.H., Ingvaldsen R., Nilsen J.E.Ø. & Skagseth Ø. 2010. Barents Sea heat-transport, storage and surface fluxes. *Ocean Science 6*, 291–234.

Steele M., Morison J.H. & Curtin T.B. 1995. Halocline water formation in the Barents Sea. *Journal of Geophysical Research—Oceans 100*, 881–894.

Sundfjord A., Fer I., Kasajima Y. & Svendsen H. 2007. Observations of turbulent mixing and hydrography in the marginal ice zone of the Barents Sea. *Journal of Geophysical Research—Oceans 112*, C05008, doi: 10.1029/2006JC003524.

Sutton R.T. & Hodson D.L.R. 2005. Atlantic forcing of the North American and European summer climate. *Science 309*, 115–118.

Tereščenko V.V. 1997. *Sezonnye i mežgodovye izmenenija temperatury i solenosti vody osnovniyh tecenij na razreze "Kol'skij meridian" v Barencevom More. (Seasonal and year-to-year variation in temperature and salinity of the main currents along the Kola section in the Barents Sea.)* Murmansk: Knipovich Polar Research Institute of Marine Fisheries and Oceanography.

Uppala S., Dee D., Kobayashi S., Berrisford P. & Simmons A. 2008. Towards a climate data assimilation system: status update of ERA-Interim. *ECMWF Newsletter 115*, 12–18.

van Gastel P. & Pelegrí J.L. 2004. Estimates of gradient Richardson numbers from vertically smoothed data in the Gulf Stream region. *Scientia Marina 68*, 459–482.

Citation: *Polar Research* 2013, *32*, 18905, http://dx.doi.org/10.3402/polar.v32i0.18905